


## Optimizing synchrony with a minimal coupling strength of coupled phase oscillators on complex networks based on desynchronous clustering

Wei Chen<sup>1</sup>, Jian Gao<sup>1</sup>, Yueheng Lan<sup>1</sup>, and Jinghua Xiao<sup>1,2,\*</sup>

<sup>1</sup>*School of Science, Beijing University of Posts and Telecommunications, Beijing 100876, China*

<sup>2</sup>*State Key Lab of Information Photonics and Optical Communications, Beijing University of Posts and Telecommunications, Beijing 100876, China*

 (Received 6 November 2021; revised 9 January 2022; accepted 9 March 2022; published 1 April 2022)

Finding the globally optimal network is an unsolved problem in synchrony optimization. In this paper, an efficient edge-adding optimization method based on global information is proposed. The edge-adding scheme is obtained through the eigenvector corresponding to the maximum eigenvalue of the system's Jacobian matrix. With different frequency distributions, we find that the optimized networks have similar features, concluded as three conditions: (i) The deviations of nodes' frequencies from the mean value are linear with the nodes' degrees, (ii) the oscillators form a bipartite network divided according to the frequencies of the oscillators, and (iii) oscillators are only connected to those with sufficiently large frequency differences. An optimal network can be constructed directly based on these three conditions for a given distribution of natural frequencies. We show that the critical coupling strengths of these constructed networks approach the theoretical lower bound. The constructed networks are or at least close to the globally optimal ones for synchrony.

DOI: [10.1103/PhysRevE.105.044302](https://doi.org/10.1103/PhysRevE.105.044302)

### I. INTRODUCTION

Synchronization, as one of the commonly observed collective behavior in coupled oscillators, has been a hot topic in nonlinear science because it is related to diverse generic mechanisms of self-organization and has wide applications, such as neuronal computation and pacemakers [1,2]. The most successful paradigm for studying synchronization of coupled oscillators is the Kuramoto model introduced in 1975 [3], which has been used to explain the emergence of collective motion in many different areas of science and technology [4–7], such as electrochemical oscillators [8], flashing fireflies [9], arrays of lasers [10,11], power grids [12–14], Josephson junctions [15,16], etc.

The classical Kuramoto phase oscillator model reads

$$\dot{\theta}_i = \omega_i + \frac{k}{\langle d \rangle} \sum_{j=1}^N A_{ij} \sin(\theta_j - \theta_i), \quad i = 1, 2, \dots, N, \quad (1)$$

where  $\theta_i$  and  $\omega_i$  are the phase and natural frequency of the  $i$ th oscillator.  $k$  is the coupling strength, and  $A$  is the adjacency matrix with  $A_{ij} = 1$  if node  $i$  and node  $j$  have a connection, otherwise  $A_{ij} = 0$ .  $d_i$  is the degree of the  $i$ th oscillator, and  $\langle d \rangle = \sum_{i=1}^N d_i / N$  is the average value.

To measure the state of the system, the order parameter  $R$  is defined as  $R = \langle r(t) \rangle_T$ , with

$$r(t)e^{I\psi(t)} = \frac{1}{N} \sum_{j=1}^N e^{I\theta_j(t)}, \quad (2)$$

where  $\langle \dots \rangle_T$  is time average over a large time span  $T$  and  $I = \sqrt{-1}$ .  $R \in [0, 1]$  measures the phase coherence of oscillator populations. When  $R \rightarrow 1$ , the system reaches a completely synchronous state, and when  $R \rightarrow 0$ , the oscillators exhibit incoherence and behave almost independently.

Considerable research has shown that the underlying structure of a network plays a crucial role in determining synchronization [17–24]. Synchrony optimization [25,26] is to promote the system's synchronization by adjusting network structure and node's frequency. Previous optimization procedures [27–31] are carried out by checking the order parameter, maximizing the synchronization degree  $R$  of the final synchronous state. However, in the synchronous state,  $R$  is close to 1. The optimization easily goes awry in the presence of noise and is thus not robust. Therefore, synchrony optimization considered in this paper is from another angle, synchronizing a system with minimal coupling strength. This is inspired by and closely related to applications such as the synchronous swing of power grid [32–34]. Hence, in this paper we try to minimize the critical coupling strength of synchronization. The critical coupling strength is negatively correlated with the order parameter  $R$ . The smaller the critical coupling strength, the greater the system order parameter  $R$  with the same coupling strength. Therefore, the optimization of the critical coupling strength in this paper is consistent with optimizing the order parameter  $R$ . With the optimization, the system can achieve synchronization under smaller coupling strengths, which is also related to synchronous control [35,36]. However, unlike the general synchronous control, which requires a time-dependent input, our method only changes the network structure.

The aim of the paper is to obtain a globally optimal network that minimizes the critical coupling strength. At present,

\*jhxiao@bupt.edu.cn

an analytic formula of the critical coupling strength of coupled oscillators on complex networks is not obtainable in general. It is difficult to analyze the synchronization directly from the coupling strength. Through numerical simulations, we find that adding edges between different partial synchronization groups can effectively reduce the critical coupling strength. Based on this fact, we develop an edge-adding optimization scheme, where edges are added to connect the two components with the largest difference of the eigenvector for maximum eigenvalue of the Jacobian matrix. By analyzing the characteristics of the optimized network, this paper summarizes three conditions, for its construction with a given distribution of natural frequencies.

The remainder of this paper is organized as follows. In Sec. II, we introduce the optimization scheme based on the clustering of asynchronous groups. In Sec. III, with different distributions of frequencies, a network is optimized by adding edges. The characteristics of the optimized network are obtained, and demonstrated in examples of synchronization optimization. Concluding remarks are made in Sec. IV.

## II. OPTIMIZATION METHOD

In this paper, we focus on the desynchronization process. The initial state of the oscillators are prepared in the complete synchronization state with sufficiently large coupling strength. We gradually decrease the coupling strength to the critical coupling strength, when the system splits into multiple groups. To reduce the critical coupling strength, one obvious strategy is to suppress the splitting. The simplest way is to add edges between the groups split first. The following is a simple example to verify. Consider adding edges on a ring network of 11 nodes, whose natural frequencies are linearly and evenly distributed on  $[0,1]$ , as shown in Fig. 1(a). The values in the dots represent the nodes' natural frequencies. Based on numerical simulations of Eq. (1), the desynchronization process with a decrease of the coupling strength is shown in Fig. 1(b), being a bifurcation diagram of nodes' average frequencies. When the coupling strength  $k$  is large ( $k = 1.5$ ), the system is in complete synchronization. Then the coupling strength is gradually reduced. At the critical coupling strength  $k_c = 1.24$ , the system is divided into two groups, marked with green and red, respectively, shown in Figs. 1(a) and 1(b).

Figure 1(c) shows three different ways to add edge connection to the network denoted as (G-G), (G-R), and (R-R). For the connection (G-G), there are 15 ways that edge connections are added within the green group. For (G-R) there are 28 cases between the green and red groups; as for (R-R) there are three within the red group. The mean and variance of the network's critical coupling strength after adding an edge are shown in Fig. 1(d). It is found that in (G-G) and (R-R), adding an edge within the synchronous group increases the critical coupling strength of the system, while for (G-R), adding an edge between the green and red groups reduces the critical coupling strength of the system. Besides, the variance of the coupling strength for the approach (G-R) is large. Even if the edge is added between groups, the effect is different for different pairs. Therefore, it is necessary to select an appropriate pair to put a new edge between groups.

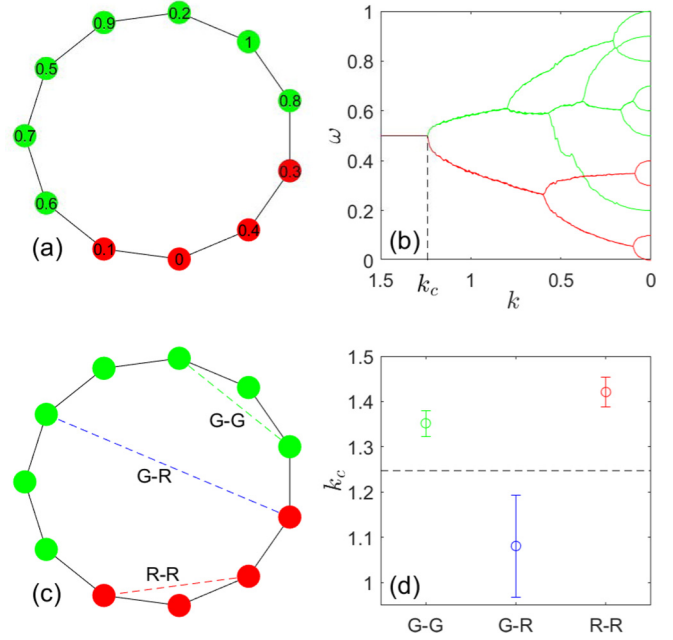


FIG. 1. (a) A ring network with 11 nodes; the values in the dot represent the nodes' natural frequencies, and the red and green color of the node represents the clustering after the splitting. (b) The bifurcation of nodes' average frequencies with the decrease of coupling strength. (c) There are three different ways to add edge: (G-G) edge is added within the green group, (G-R) edge is added between the green and the red groups, (R-R) edge is added within the red group. (d) The mean and variance of the network's critical coupling strength after adding an edge in three different ways, and the black dotted line corresponds to the critical coupling strength of the initial network.

Let the phase of the complete synchronization be  $\bar{\theta}^*$  and the Jacobian matrix of Eq. (1) be  $J$ :

$$J_{ij} = \frac{k}{\langle d \rangle} A_{ij} \cos(\theta_j - \theta_i), \quad i \neq j$$

$$J_{ii} = -\frac{k}{\langle d \rangle} \sum_{j=1}^N A_{ij} \cos(\theta_j - \theta_i). \quad (3)$$

Let  $\lambda_j$  and  $\vec{v}^j$  be the eigenvalues and eigenvectors of the Jacobian matrix. From the linear stability analysis, a disturbance near the fixed point of the synchronization:  $\bar{\theta} = \bar{\theta}^* + \vec{\xi}$ , the evolution of which  $\vec{\xi}(\vec{\xi}(0) = \sum_{j=1}^N a_j \vec{v}^j)$  is

$$\vec{\xi}(t) = \sum_{j=1}^N a_j e^{\lambda_j t} \vec{v}^j. \quad (4)$$

When the coupling strength is  $k = k_c - \varepsilon$ ,  $0 < \varepsilon \ll 1$ , the system is unstable, and the maximum eigenvalue of Jacobian matrix  $J$  is greater than 0 [37]. The row sum of Jacobian matrix  $J$  is 0, so the constant is the eigenvector of  $J$  corresponding to the eigenvalue 0. Assuming that the eigenvalues satisfy  $\lambda_1 \leq \lambda_2 \leq \dots \leq \lambda_{N-1} = 0 < \lambda_N$ , when  $t$  is large, the disturbance  $\vec{\xi}(t)$  is

$$\vec{\xi}(t) = a_{N-1} \vec{v}^{N-1} + a_N e^{\lambda_N t} \vec{v}^N \approx a_N e^{\lambda_N t} \vec{v}^N. \quad (5)$$

The phase deviation is proportional to the eigenvector  $\bar{v}^N$  corresponding to the largest eigenvalue  $\lambda_N$ . Therefore, in the edge-adding optimization, edges should be added between the nodes corresponding to the two components that have the largest difference in vector  $\bar{v}^N$ . To obtain  $\bar{v}^N$ , we need to calculate the critical coupling strength  $k_c$  and the corresponding phase  $\bar{\theta}^*$ . However, an exact analysis of the critical coupling strength in complex networks is still an unsolved problem. An efficient iteration procedure for calculating the critical coupling strength is given in Appendix A. In Appendix B, we further develop an estimation method for oscillators' phases near the critical coupling strength, which needs less calculation than in Appendix A.

After the phase  $\bar{\theta}^*$  and the critical coupling strength  $k_c$  are obtained from Appendix A or B, according to Eq. (3), the Jacobian matrix  $J$  can be obtained as well as all its eigenvalues and eigenvectors. Following the optimization above, we identify the two components  $i$  and  $j$  with the largest difference in  $\bar{v}^N$ , and add an edge between  $i$  and  $j$  if there is no edge connection between them (i.e.,  $A_{ij} = 0$ ). If there is already an edge between nodes  $i$  and  $j$ , we will search the two components with the second largest difference in  $\bar{v}^N$ . The optimization results obtained by the methods in Appendix A or B are basically the same. In this paper, the method with less calculation in Appendix B is used except for the case where it is necessary to accurately calculate the critical coupling strength  $k_c$ .

Similar to the edge-adding optimization, one can consider the edge breaking, which is also popular in recent researches [30,31]. Following our approach, when considering edge breaking, one should find the two components with the smallest difference in  $\bar{v}^N$ . However, such components are significantly affected by random factors such as disturbance and thus not robust. Therefore, the edge-adding optimization is hence used in this paper.

This paper considers the simplest edge-adding scheme on undirected and weightless networks. In practice, there will be different constraints. As a simple example, when there are unconnected edges. Let  $B$  be the complement of the adjacency matrix  $A$  (if the edges between nodes  $i$  and  $j$  cannot be connected,  $B_{ij} = 1$ , otherwise  $B_{ij} = 0$ ). After obtaining the eigenvector  $\bar{v}^N$  corresponding to the maximum eigenvalue of Jacobian matrix  $J$ , find the node  $i$  and  $j$  corresponding to the two components with the largest difference in  $\bar{v}^N$ . If there is no edge connection between nodes  $i$  and  $j$  ( $A_{ij} = 0$ ) and nodes  $i$  and  $j$  can be connected ( $B_{ij} = 0$ ), add an edge between nodes  $i$  and  $j$ , otherwise find the two components with the second largest difference in  $\bar{v}^N$  for judgment. The improvement of the current method with different constraints is another research topic for future investigation.

### III. NETWORK OPTIMIZATION AND GLOBAL OPTIMAL NETWORK

In order to test the above optimization technique, three edges are added to the Watts-Strogatz (WS) network ( $N = 30$ ,  $p = 0.1$ ), the structure of which is displayed in Fig. 2(a). Green dots are network nodes in which the numbers mark natural frequencies, while black solid lines constitute the original

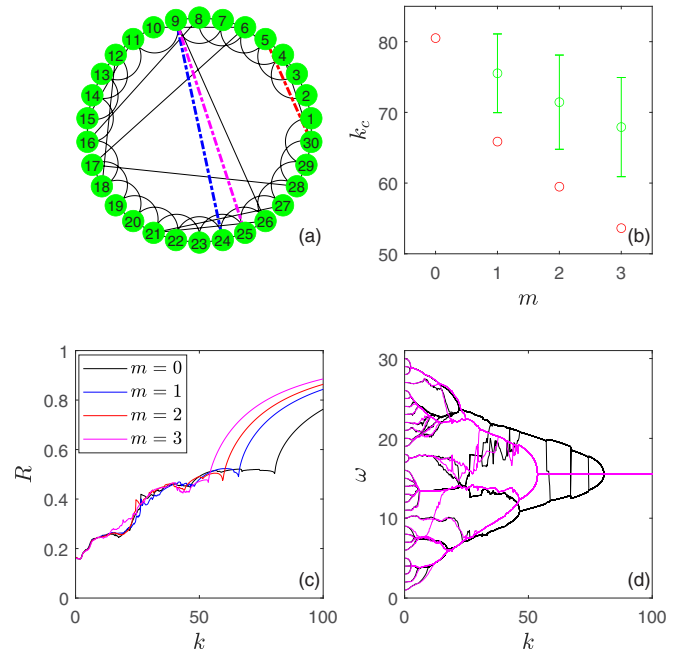


FIG. 2. (a) The network structure; (b) the critical coupling strength  $k_c$  vs the number of adding edges  $m$ ; (c) the order parameter  $R$  vs coupling strength  $k$  at  $m = 0, 1, 2, 3$ ; (d) the bifurcation of nodes average frequency. The black line is the original plot, and the mauve line is the case after adding three edges.

WS network. The first added edge is a blue dotted line, the second is a red dotted line, and the third is a mauve dotted line. The variation of the critical coupling strength  $k_c$  with the number of added edges  $m$  is shown as red circles in Fig. 2(b). The green error bars in Fig. 2(b) plot variations for randomly supplying edges. When  $m = 1$ , all possible cases (375 kinds) are considered. When  $m = 2$ , two edges are randomly added and the process is repeated 100 000 times, and similarly for  $m = 3$ . The mean and mean square deviation of the critical coupling strength are obtained, as shown by the green error bars. It is found that the edge adding based on desynchronous clustering is much better than that based on random picking. Figure 2(c) shows the variation of the order parameter  $R$  with the coupling strength  $k$  at  $m = 0, 1, 2, 3$ . It is found that the order parameter  $R$  increases significantly with the increase of  $m$ , which shows that the optimal synchronization to reduce the critical coupling strength  $k_c$  is consistent with the one of increasing  $R$ . Figure 2(d) shows the bifurcation of node average frequency. The black line is the original plot, and the mauve line is the case after adding three edges.

In the following, we consider the edge-adding optimizing in sparse networks, which is exercised on an Erdős-Rényi (ER) network [38] with the edge connection probability  $p = 0.04$  and the node number  $N = 100$ . The natural frequencies  $\omega_i = (i - 1)/(N - 1)$  are linearly and uniformly distributed on  $[0, 1]$ . For each additional 25 edges (the average degree of the network increases by 0.5), the critical coupling strength is calculated by the method in Appendix A. We do the edge-adding optimization from 100 different initial ER networks, and the optimization results are shown in Fig. 3, in which (a) and (b) depict the dependence of the average critical coupling

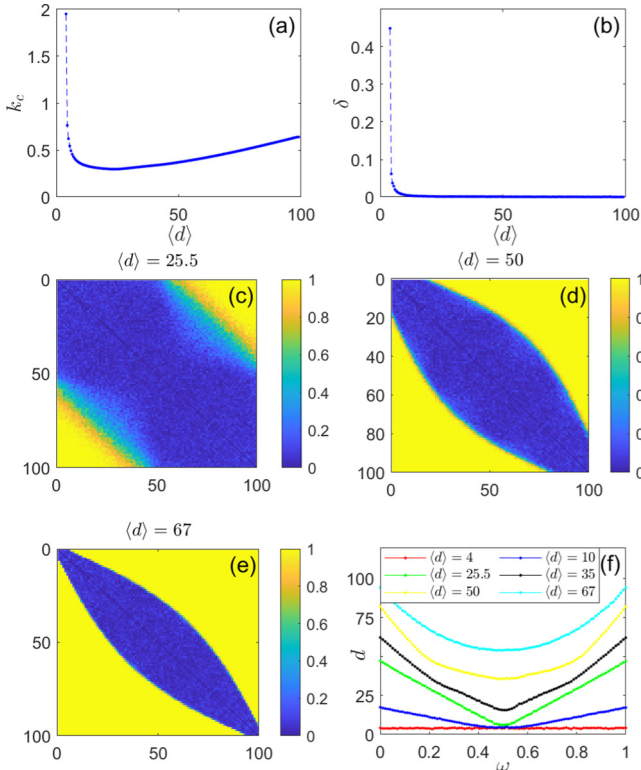


FIG. 3. Synchronization optimization with uniform frequency distribution on ER networks. (a) The average critical coupling strength  $k_c$  vs the average degree  $\langle d \rangle$ . (b) The variance  $\delta$  vs mean  $\langle d \rangle$ . (c)–(e) The connection probability matrix corresponding to  $\langle d \rangle = 25.5$ ,  $\langle d \rangle = 50$ , and  $\langle d \rangle = 67$ , respectively. (f) The corresponding relationship between the frequency and degree of the connection probability matrix with different average degrees  $\langle d \rangle$ .

strength  $k_c$  and its variance  $\delta$  on the network's average degree. It is found that the critical coupling strength  $k_c$  decreases first and then increases with the average degree  $\langle d \rangle$ . The minimum value of  $k_c$  is obtained at  $\langle d \rangle = 25.5$ . It can be seen from Fig. 3(b) that the variance  $\delta$  decreases fast to near 0, indicating that the networks obtained from different ER networks tend to be consistent in the edge-adding optimization. The adjacency matrices of 100 networks with the same number of edges supplied are superimposed and averaged to compute the connection probability. Figures 3(c)–3(e) displays the connection probability matrix corresponding to  $\langle d \rangle = 25.5$ ,  $\langle d \rangle = 50$ , and  $\langle d \rangle = 67$ , respectively. The color of each point in the figure represents the probability of edge connection of the corresponding nodes. The edges added are mainly in the yellow area far away from the diagonal corresponding to the nodes with large frequency differences, which are preferentially connected during optimization. However, it can be seen from Figs. 3(d) and 3(e) that the boundary line of the yellow area is not parallel to the diagonal, so the edges are not added completely according to the frequency difference. Figure 3(f) shows the corresponding relationship between the frequency and degree of nodes. It is found that the absolute frequency deviation from the average in the optimized network is positively correlated with its degree. Specifically, in

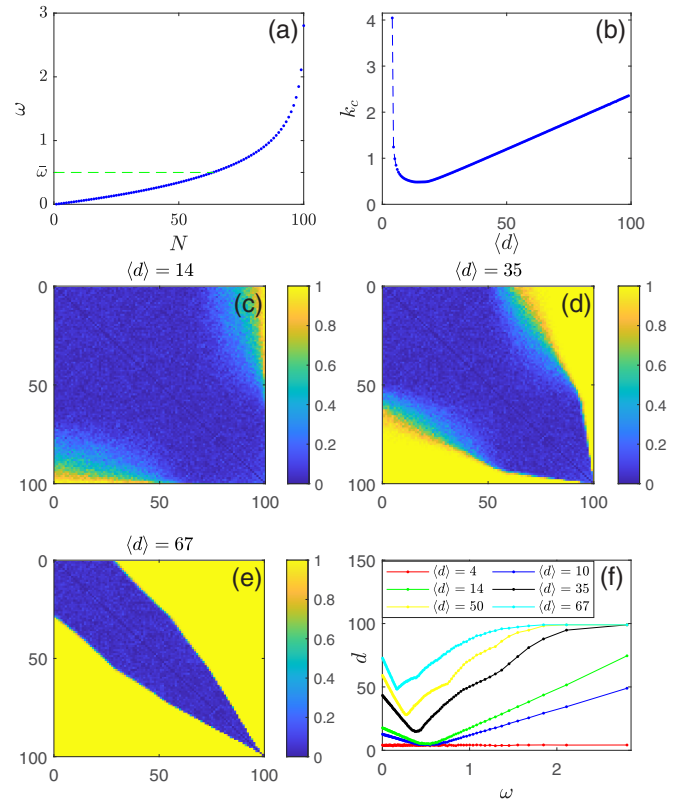


FIG. 4. Synchronization optimization with exponential frequency distribution on ER networks. (a) The natural frequency value of the node. (b) The average critical coupling strength  $k_c$  vs average degree  $\langle d \rangle$ . (c)–(e) The connection probability matrix corresponding to  $\langle d \rangle = 14$ ,  $\langle d \rangle = 35.5$ , and  $\langle d \rangle = 67$ , respectively. (f) The corresponding relationship between the frequency and degree of the connection probability matrix under different average degrees  $\langle d \rangle$ .

the low-density network with  $\langle d \rangle \leq 25.5$ , we have a linear relation  $|\omega_i - \bar{\omega}|/d_i \approx |\omega_j - \bar{\omega}|/d_j$ .

Different natural frequency distributions will have vastly different impacts on the results. For example, in the synchronous echo phenomenon [39,40], the results are highly sensitive to the frequency distribution used. Therefore, we need to consider different natural frequency distributions. When the natural frequency of the node is asymmetric, following an exponential distribution, for example, the above 100 ER random networks with  $p = 0.04$  and  $N = 100$  can also be optimized by supplying additional edges. The results are shown in Fig. 4. Figure 4(a) shows the nodes' natural frequencies. The green dotted line indicates the average frequency  $\bar{\omega}$ . Figure 4(b) shows the average critical coupling strength  $k_c$  vs the average degree  $\langle d \rangle$ . The derived average critical coupling strength decreases first and then increases. The minimum value of  $k_c$  is obtained at  $\langle d \rangle = 14$ . Figures 4(c)–4(e) shows the connection probability matrix corresponding to  $\langle d \rangle = 14$ ,  $\langle d \rangle = 35.5$ , and  $\langle d \rangle = 67$ , respectively. It is found that the yellow area is still far from the diagonal. Affected by the frequency asymmetry, the optimized network is no longer as symmetrical as that in Fig. 3. Figure 4(f) shows the relationship between the nodes' frequencies and degrees with different average degrees  $\langle d \rangle$ . It is found that when the average



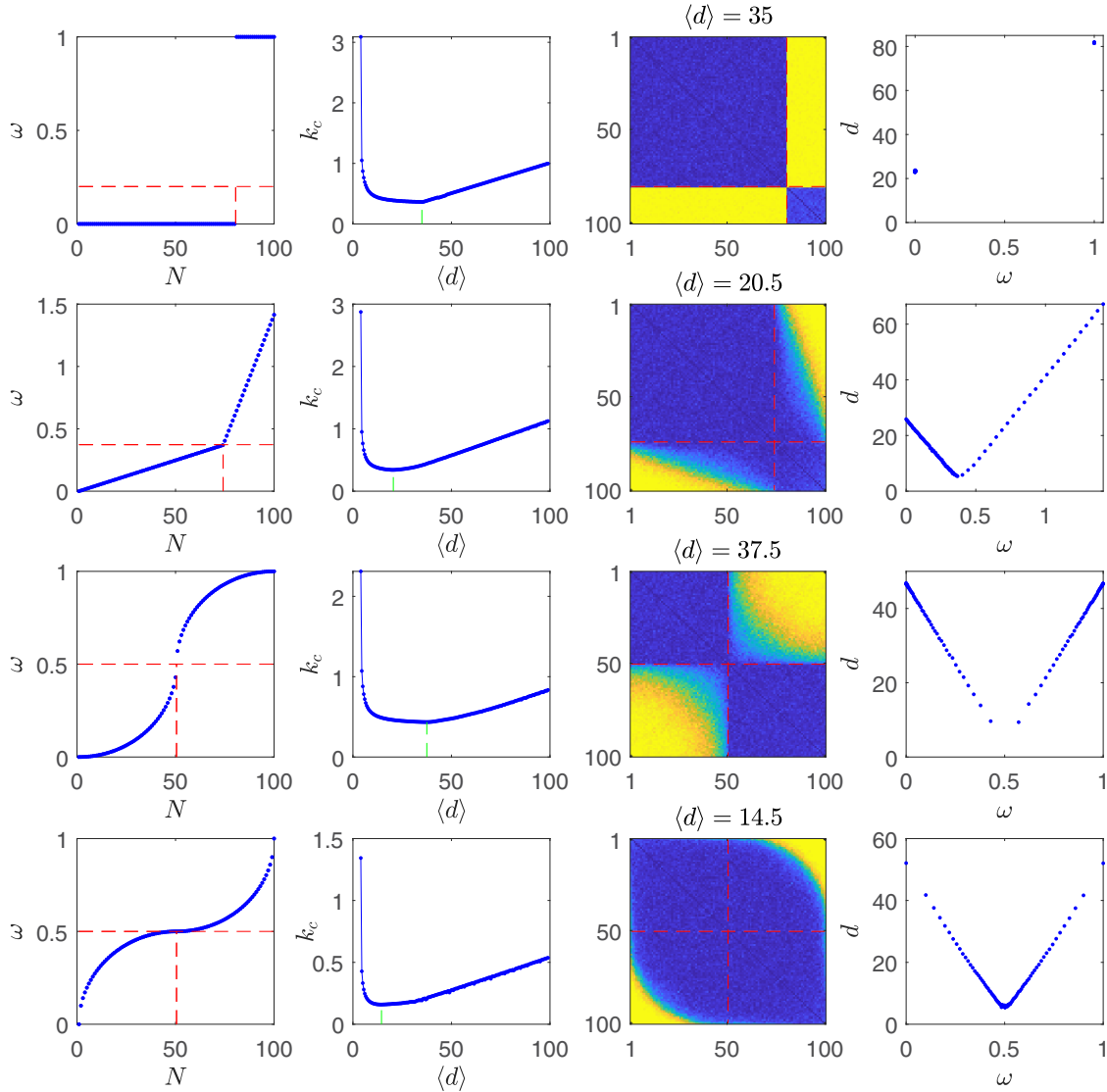


FIG. 5. The optimization results of adding edge connection with four different distributions of natural frequencies. The first column is the frequency distribution. The second column shows the average critical coupling strength  $k_c$  vs the average degree  $\langle d \rangle$ , the minimum of which is marked with a green dotted line. The third column is the connection probability matrix corresponding to the minimum critical coupling strength. The fourth column is the correspondence between the node frequency and the degree of the connection probability matrix corresponding to the third column.

degree  $\langle d \rangle$  is small, the node's absolute frequency deviation from the average is linear with the degree:  $|\omega_i - \bar{\omega}|/d_i \approx |\omega_j - \bar{\omega}|/d_j$ . With the increase of  $\langle d \rangle$ , the frequency of the node with the smallest degree will shift to the left of  $\bar{\omega}$ .

From the above results, it can be seen that there is an optimal number of edges to minimize the critical coupling. When the natural frequency is uniformly distributed, it can be seen from Fig. 3(d) that the network is basically close to a bipartite network. Nodes with serial numbers less than 50 are basically connected to nodes with serial numbers greater than 50. The slots with 1 in the adjacency matrix basically stand together and away from the diagonal. Looking at the green line in Fig. 3(f), we can see that the node's absolute frequency deviation from the average is linear with the degree. When the natural frequency is exponentially distributed, it can be seen from Figs. 4(c) and 4(f) that the characteristics of the optimal network are similar.

For other distributions of natural frequencies, the results are similar, as shown in Fig. 5. It is found that all the optimal networks basically have similar properties: (i) The deviations of node frequencies from the mean value are linear with the nodes' degrees; (ii) the oscillators form a bipartite network where the ones with lower or higher frequencies are divided into two groups; (iii) the region with the adjacency matrix of 1 exists as a cluster and is far away from the diagonal, meaning that the oscillators are connected to all the other ones with sufficiently large frequency differences.

Through the optimization, optimized networks have a memory of the initial networks. In addition, we can directly construct the network based on the above properties. First, consider the simplest case. The frequency is linear and uniform:  $\omega_i = (i - 1)/(n - 1)$ . The network constructed is shown in Fig. 6(a). We will show that in some cases these constructed networks can approach the optimal networks with the

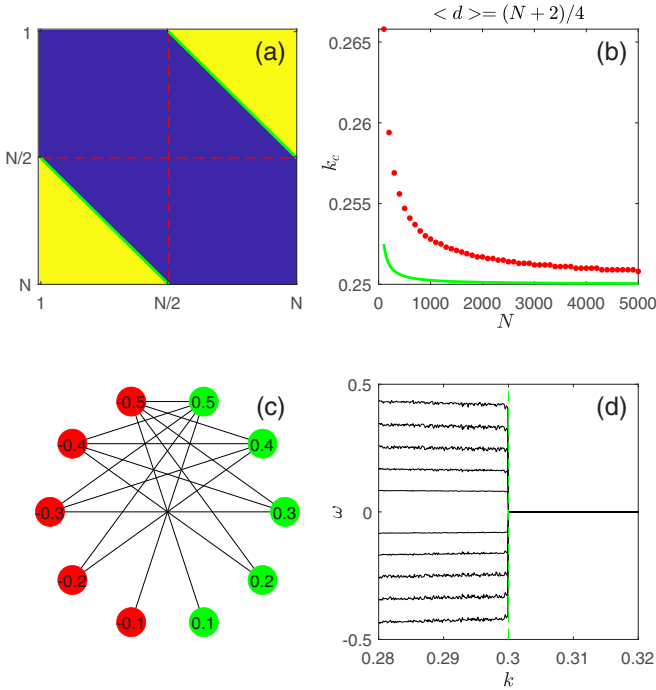


FIG. 6. (a) When the frequency  $\omega_i = (i - 1)/(n - 1)$ , the adjacency matrix of the optimal network is constructed. (b) The comparison between the critical coupling strength  $k_c$  (red solid dot) and the theoretical lower bound  $k_m$  (green solid line) at different network sizes  $N$ . (c) The network constructed at  $N = 10$ ,  $\bar{\omega} = [-0.5, -0.4, -0.3, -0.2, -0.1, 0.1, 0.2, 0.3, 0.4, 0.5]^T$ . (d) The dependence of the instantaneous average frequencies on the coupling strength  $k$ . Here, the critical coupling strength is deduced from the synchronous state and recorded by quasistationary method.

theoretical minimum value of the critical coupling strength  $k_c$ . When the system is fully synchronized,  $\dot{\theta}_i = \bar{\omega}$ , the condition for the coupling strength  $k$  can be obtained from Eq. (1):

$$k = \frac{|\omega_i - \bar{\omega}| \langle d \rangle}{\left| \sum_{j=1}^N A_{ij} \sin(\theta_j - \theta_i) \right|} \geq \frac{|\Omega_i| \langle d \rangle}{d_i}, \quad i = 1, 2, \dots, N, \quad (6)$$

where  $\Omega_i = \omega_i - \bar{\omega}$ . At the critical point  $k = k_c$ , the system is also fully synchronized. Hence, we have  $k_c \geq |\Omega_i| \langle d \rangle / d_i$ , which can be further simplified:

$$k_c \geq \max_i \left( \frac{|\Omega_i| \langle d \rangle}{d_i} \right) \geq \frac{\sum_{i=1}^N |\Omega_i| \langle d \rangle}{\sum_{i=1}^N d_i} = \sum_{i=1}^N \frac{|\Omega_i|}{N}. \quad (7)$$

The above expression takes the equal sign when  $|\Omega_i|/d_i = |\Omega_j|/d_j$ ,  $i, j = 1, 2, \dots, N$  which corresponds to the previous condition (i): The absolute frequency difference with respect to the average is linear with the node's degree. The lower bound of  $k_c$  is denoted as  $k_m$ ,

$$k_m = \sum_{i=1}^N \frac{|\Omega_i|}{N}, \quad (8)$$

which is determined by the distributions of natural frequencies and independent of the average degree of the network. Figure 6(b) shows the comparison between the critical coupling strength  $k_c$  of the constructed network and the theoretical lower bound  $k_m$  at different network sizes  $N$ . It is

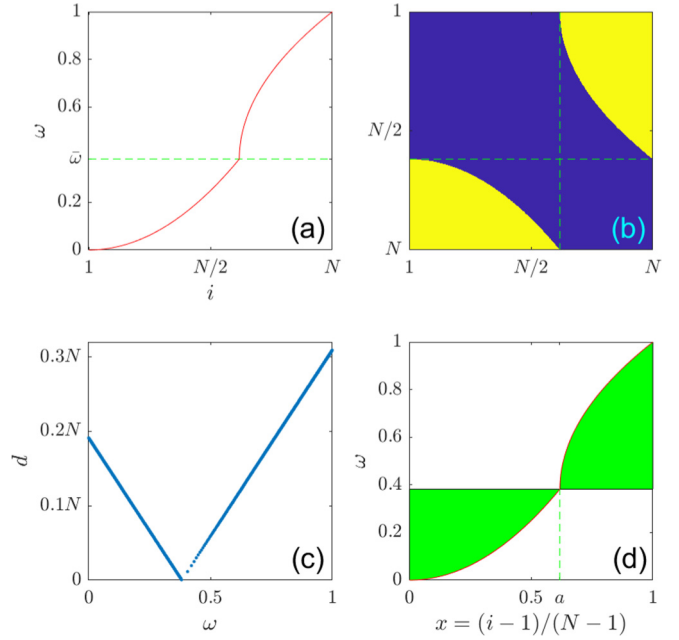


FIG. 7. (a) Frequency value. (b) Adjacency matrix of the constructed network. (c) The functional dependence of the frequency on the node degree. (d) The node serial number is rescaled to  $[0, 1]$ :  $x_i = (i - 1)/(n - 1)$ , and the distance from the frequency to the average is represented by the green area.

found that the difference between  $k_c$  and  $k_m$  is very small. Besides, with the increase of the network size  $N$ , the critical coupling strength  $k_c$  can approach the lower bound  $k_m$ . In fact,  $k_c$  and  $k_m$  cannot be equal because  $d_i$  must be rounded, resulting in a small difference between  $|\Omega_i|/d_i$  and  $|\Omega_j|/d_j$ . Hence, the second equal sign in the equality Eq. (7) cannot hold. Increasing  $N$  reduces the difference between  $|\Omega_i|/d_i$  and  $|\Omega_j|/d_j$  caused by rounding  $d_i$ . Therefore, with the increase of network scale  $N$ , the critical coupling strength  $k_c$  approaches the lower bound  $k_m$ . It is also possible to fine tune the value of frequency  $\bar{\omega}$  to make  $|\Omega_i|/d_i$  and  $|\Omega_j|/d_j$  exactly equal. Consider a simple case:  $N = 10$ , frequency  $\bar{\omega} = [-0.5, -0.4, -0.3, -0.2, -0.1, 0.1, 0.2, 0.3, 0.4, 0.5]^T$ . The network constructed in a manner similar to Fig. 6(a) is shown in Fig. 6(c). Figure 6(d) shows the change of average frequency with the coupling strength. Here, the critical coupling strength is deduced from the synchronous state and recorded by quasistationary method. It is found that the critical coupling strength  $k_c$  is equal to the lower bound  $k_m$ , both of which are 0.3. It can be seen from the above analysis that the critical coupling strength of the network constructed in Fig. 6(a) can approach its theoretical lower bound, which corresponds to a uniform distribution of natural frequencies.

We may construct the globally optimal network according to the three conditions (i–iii), but not all distributions of frequencies satisfy the three conditions at the same time. There is a symmetry condition for the distributions as illustrated by an example in Fig. 6. In Fig. 7(d), the node serial number is rescaled to  $[0, 1]$ :  $x_i = (i - 1)/(n - 1)$ , and the distance to the average frequency is represented by the green area. Because the adjacency matrix is a symmetric matrix about the diagonal, the shapes of the two yellow regions in Fig. 7(b)

should be the same. Since the frequency in Fig. 7(c) satisfies a linear relationship, the two green areas in Fig. 7(d) and the two yellow areas in Fig. 7(b) should be symmetrical, that is, the shapes of the two green areas in Fig. 7(d) should be the same. Let the frequency value function be  $G(x): \omega_i = G(x_i) = G((i-1)/(n-1))$ , then the graph of  $G(x)$  in section  $x \leq a$  and that in section  $x \geq a$  make up the profiles of a function and its inverse. Therefore, the frequency function  $G(x)$  needs to satisfy

$$G(x) = \begin{cases} g(x), & x \leq a \\ g(a) + bg^{-1}(x-a), & x > a \end{cases} \quad (9)$$

where  $b$  is the amplification or the reduction factor of frequencies. Discomfort general order  $g(0) = 0$ . In the following, let  $b = 1$ . Hence the frequency range is  $[0, 1]$ . Because the average frequency reads  $\bar{\omega} = G(a)$ , the value of  $a$  shall satisfy

$$\begin{aligned} \bar{\omega} = g(a) &= \int_0^1 G(x) dx \\ &= \int_0^a g(x) dx + \int_a^1 g(a) + b * g^{-1}(x-a) dx. \end{aligned} \quad (10)$$

The optimal network can be constructed for the distributions of frequencies satisfying the conditions Eqs. (9) and (10). Given the node's frequency  $\omega$ , let its degree be  $d_i = [N|\omega_i - \bar{\omega}|]$ , where  $[x]$  takes the integer part of  $x$ . Then the value of adjacency matrix  $A$  can be constructed as follows:

$$\begin{aligned} A_{ij} &= 1, & j \geq N + 1 - d_i, & \Omega_i \leq 0 \\ A_{ij} &= 0, & j < N + 1 - d_i, & \Omega_i \leq 0 \\ A_{ij} &= 1, & j \leq d_i, & \Omega_i > 0 \\ A_{ij} &= 0, & j > d_i, & \Omega_i > 0 \end{aligned}, \quad i = 1, \dots, N. \quad (11)$$

Two examples are shown in Fig. 8. The first row of Fig. 8 shows the frequency value:  $\omega_i = G(x_i) = G((i-1)/(N-1))$ , with the case  $g(x) = cx$ ,  $b = 1$ ,  $a = 1/(c+1)$  corresponding to Fig. 8(a), and the case  $g(x) = \sqrt{0.25 - (x - 0.25)^2}$ ,  $b = 1$ ,  $a = 0.5$  corresponding to Fig. 8(b). The second row of Fig. 8 shows the optimal network constructed according to Eq. (11). The third row of Fig. 8 shows the critical coupling strength  $k_c$  and theoretical lower bound  $k_m$  as a function of the network scale  $N$ . It is found that the critical coupling strength of the constructed network is gradually approaching the theoretical minimum, but there is still a difference between them.

In order to verify whether the network constructed by the above method is globally optimal, we randomly change one edge of the network, that is, randomly disconnect one edge and then randomly connect another. It is interesting to check the change of critical coupling strength of the system after this switch. For the constructed network in Fig. 8(d), we make this random change 100 000 times, and obtain the distribution of 100 000 critical coupling strengths, as shown in Fig. 9. The blue line in the figure corresponds to the critical coupling strength of the network in Fig. 8(d). It is found that changing one edge randomly will increase the critical coupling of the system. It is numerically verified that the constructed network structure is a global optimal network structure.

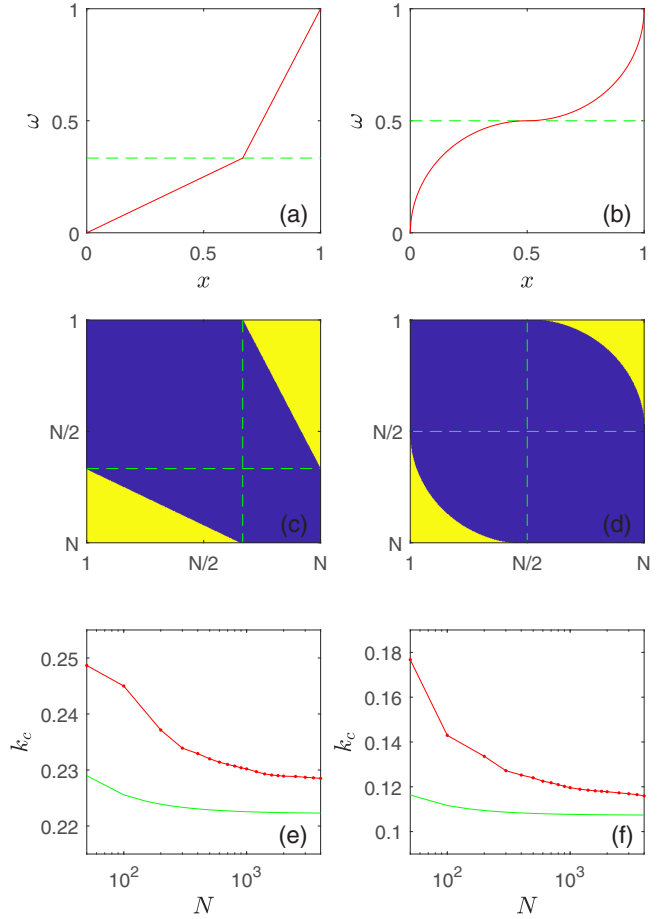


FIG. 8. Two examples of an optimal construction. The first row shows the frequency value:  $\omega_i = G(x_i) = G((i-1)/(N-1))$ . (a)  $g(x) = 0.5x$ ,  $b = 1$ ,  $a = 2/3$ . (b)  $g(x) = \sqrt{0.25 - (x - 0.25)^2}$ ,  $b = 1$ ,  $a = 0.5$ . The second row shows the optimal network constructed according to Eq. (11). The third row shows the variation of the critical coupling strength  $k_c$  (red solid line) and theoretical lower bound  $k_m$  (green solid line) with the network sizes  $N$ .

When the distribution of frequencies does not satisfy Eq. (9), the matrix constructed by Eq. (11) is not a symmetric matrix and cannot correspond to the adjacency matrix of a network. Therefore, the optimal network cannot meet the three conditions (i), (ii), and (iii) at the same time. In this case, is there a network whose critical coupling strength  $k_c$  approaches the lower bound  $k_m$ ? How does one find it? A network satisfying conditions (i) and (ii) can be constructed, however. The nodal degree  $d_i = [N|\omega_i - \bar{\omega}|]$  is obtained from condition (i). Condition (ii) requires that nodes  $i$  and  $j$  that satisfy  $(\omega_i - \bar{\omega})(\omega_j - \bar{\omega}) \leq 0$  can be connected. Under the condition of meeting the requirements of degree and frequency of connected nodes, the network is generated by random edge connection.

#### IV. SUMMARY

In this paper, the synchronization optimization of Kuramoto oscillators on a complex network is considered. For a given frequency, we hope to obtain the optimal network

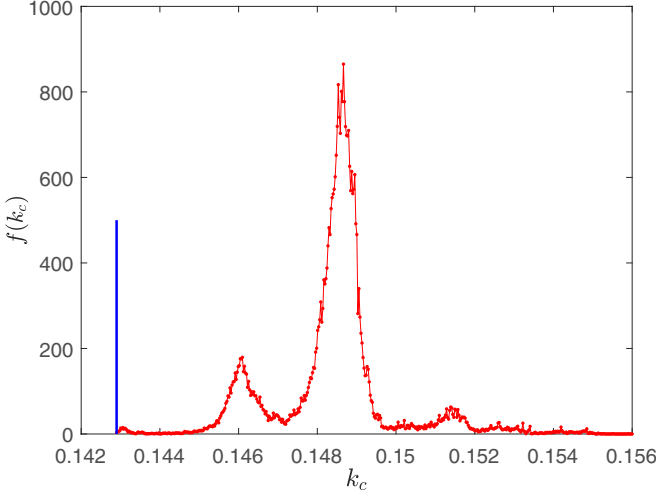


FIG. 9. For the constructed network in Fig. 8(d), one edge is randomly disconnected, and then another one is randomly added. After 100 000 repetitions, the distribution of the critical coupling strength is obtained. The blue line in the figure is the critical coupling strength of the network in Fig. 8(d).

structure to minimize the critical coupling strength. In order to obtain an efficient edge-adding optimization, the desynchronization of the system is studied. It is found that adding edges between different partial synchronization groups can effectively reduce the critical coupling strength. Specifically, an edge is added between the nodes corresponding to the two components with the largest difference of the eigenvector corresponding to the maximum eigenvalue of the Jacobian matrix near the critical coupling strength  $k_c$ . In order to calculate the Jacobian matrix  $J$  near the critical coupling strength  $k_c$ , we give two methods in the Appendix.

Using this optimization for sparse ER random networks, we find that the critical coupling strength decreases first and then increases with the average degree. At an intermediate value, we get the smallest critical coupling strength together with the optimized network. It is found that the adjacency matrix of the optimized network depends on the distribution of natural frequencies, but they should satisfy three conditions. (i) The deviations of node frequencies from the mean value are linear with the nodes' degrees. (ii) The oscillators form a bipartite network where the ones with lower or higher frequencies are divided into two groups. (iii) The region with the adjacency matrix of 1 exists as a cluster and is far away from the diagonal, meaning that the oscillators are connected to all the other ones with sufficiently large frequency differences. When the distribution of frequencies satisfies certain conditions, the network can be constructed according to condition (i)–(iii), and the critical coupling strength of the network can approach its theoretical lower bound, corresponding to the globally optimal network. For more general distribution of frequencies, optimized networks satisfying condition (i)–(ii) can be obtained.

In general, this paper proposes an effective method of synchronization optimization, and extracts characteristics of the optimized network structure. Different optimal networks are constructed for a class of natural frequencies' distributions.

The construction is not affected by the network scale. However, there are still some unsolved problems. For more general distributions of frequencies, the global optimal network structure remains elusive, which calls for further research.

#### APPENDIX A: METHOD FOR CALCULATING CRITICAL COUPLING STRENGTH

When the system is synchronized, the phase is  $\bar{\theta} = \bar{\theta}^* - \bar{\omega}t\bar{I}$ , then Eq. (1) can be written as

$$\bar{\omega} = \omega_i + \frac{k}{\langle d \rangle} \sum_{j=1}^N A_{ij} \sin(\theta_j^* - \theta_i^*), \quad (\text{A1})$$

which becomes

$$\sum_{j=1}^N A_{ij} \sin(\theta_j^* - \theta_i^*) = \frac{\langle d \rangle}{k} (\bar{\omega} - \omega_i). \quad (\text{A2})$$

When the coupling strength becomes  $k + \varepsilon$ , assuming that the system still maintains the synchronous state, and the phase  $\bar{\theta} = \bar{\theta}^* - \bar{\omega}t\bar{I} + \bar{\delta}$ , according to Eq. (1),

$$\bar{\omega} = \omega_i + \frac{k + \varepsilon}{\langle d \rangle} \sum_{j=1}^N A_{ij} \sin(\theta_j^* - \theta_i^* + \delta_j - \delta_i). \quad (\text{A3})$$

Make a first-order Taylor expansion of Eq. (A3):

$$\begin{aligned} \bar{\omega} &\approx \omega_i + \frac{k + \varepsilon}{\langle d \rangle} \sum_{j=1}^N A_{ij} \sin(\theta_j^* - \theta_i^*) \\ &\quad + \frac{k + \varepsilon}{\langle d \rangle} \sum_{j=1}^N A_{ij} \cos(\theta_j^* - \theta_i^*) (\delta_j - \delta_i). \end{aligned} \quad (\text{A4})$$

Let  $\Omega_i = \omega_i - \bar{\omega}$  and substitute Eq. (A2) into Eq. (A4) to obtain

$$J\bar{\delta} \approx \frac{\varepsilon}{k + \varepsilon} \bar{\Omega}. \quad (\text{A5})$$

The Jacobian matrix  $J$  is given in Eq. (3). Let  $\lambda_j$  and  $\bar{v}^j$  be the eigenvalues and eigenvectors corresponding to the Jacobian matrix  $J$ . When the system is in synchronous state,  $\lambda_1 \leq \lambda_2 \leq \dots \leq \lambda_{N-1} < \lambda_N = 0$ . The pseudoinverse matrix of the symmetric matrix  $J$  is  $J^\dagger = \sum_{i=1}^{N-1} \lambda_i^{-1} \bar{v}^i \bar{v}^{iT}$  [41]. Equation (A5) can be converted into

$$\frac{\bar{\delta}}{\varepsilon} \approx \frac{1}{k + \varepsilon} J^\dagger \bar{\Omega}. \quad (\text{A6})$$

When the variation  $\varepsilon$  approaches 0, Eq. (A6) is written as a differential equation:

$$\frac{d\bar{\theta}}{dk} = \frac{1}{k} J^\dagger \bar{\Omega}. \quad (\text{A7})$$

The variation of node phase  $\bar{\theta}$  with coupling strength  $k$  can be obtained by evolving Eq. (A7). Note that Eq. (A7) holds only in the synchronous state, and the coupling strength descends from a value  $k > k_c$  during the iteration. The initial phase is one corresponding to synchronization, which can be quickly obtained by solving Eq. (1). As  $k$  decreases, the second largest eigenvalue  $\lambda_{N-1}$  of  $J$  increases from a negative value. When



$\lambda_{N-1}$  increases to 0, if the coupling strength  $k$  continues to decrease, the maximum eigenvalue of  $J$  will be greater than 0, and the synchronous state of the system becomes unstable. Therefore, when the two largest eigenvalues  $\lambda_N$  and  $\lambda_{N-1}$  of  $J$  are equal to 0, the corresponding critical coupling strength  $k_c$  is reached.

The critical coupling strength of the system can be obtained by judging the two largest eigenvalues  $\lambda_N$  and  $\lambda_{N-1}$  of  $J$  upon evolving Eq. (A7). Compared with the direct numerical calculation Eq. (1), the amount of calculation is greatly reduced.

## APPENDIX B: METHOD FOR ESTIMATING CRITICAL COUPLING STRENGTH AND PHASE

Previous studies [30,36] computed the phase of each node when the coupling is strong, which will be used here to estimate phases near the critical coupling strength. When the coupling strength  $k$  is large,  $|\theta_j - \theta_i| \ll 1$ , then  $\sin(\theta_j - \theta_i) \approx \theta_j - \theta_i$ , and Eq. (1) can be transformed into a linearized equation:

$$\bar{\omega} \approx \omega_i + \frac{k}{\langle d \rangle} \sum_{j=1}^N A_{ij}(\theta_j - \theta_i). \quad (\text{B1})$$

Equation (B1) can be written in a matrix form,

$$\bar{\Omega} \approx \frac{k}{\langle d \rangle} L \bar{\theta}, \quad (\text{B2})$$

where  $\Omega_i = \omega_i - \bar{\omega}$ ,  $L(L_{ij} = -A_{ij}, L_{ii} = \sum_{j=1}^N A_{ij})$  is the Laplace matrix of the network. Let  $\gamma_j$  and  $\bar{u}^j$  be the eigenvalues and eigenvectors of  $L$ . When the network corresponding to adjacency matrix  $A$  is a connected network,  $0 = \gamma_1 < \gamma_2 \leq \dots \leq \gamma_N$ , the generalized inverse matrix of  $L$  is  $L^\dagger = \sum_{j=2}^N \gamma_j^{-1} \bar{u}^j \bar{u}^{jT}$ . According to Eq. (B2),

$$\bar{\theta} \approx \frac{\langle d \rangle}{k} L^\dagger \bar{\Omega}. \quad (\text{B3})$$

The estimated phase at different coupling strength can be obtained from Eq. (B3). Below, we explain how to estimate the critical coupling strength. Substitute the phase obtained by Eq. (B3) into Jacobian matrix  $J$  to get the eigenvalue  $\lambda^*$ . The critical coupling strength be  $k_s$  when  $\lambda_{N-1}^* + \lambda_N^* = 0$ , which is then solved by dichotomy. As a result, the estimated value  $k_s$  of critical coupling strength and the estimated phase  $\bar{\theta} \approx \langle d \rangle L^\dagger \bar{\Omega} / k_s$  are obtained.

- [1] Y. Kuramoto, *Chemical Oscillations, Waves, and Turbulence* (Springer, Berlin, 1984).
- [2] A. Pikovsky, M. Rosenblum, and J. Kurths, *Synchronization A Universal Concept in Nonlinear Sciences* (Cambridge University Press, Cambridge, 2001).
- [3] Y. Kuramoto, in *International Symposium on Mathematical Problems in Theoretical Physics*, edited by H. Araki, Lecture Notes in Physics, Vol. 39 (Springer, Berlin, 1975).
- [4] S. H. Strogatz, *Physica D* **143**, 1 (2000).
- [5] J. A. Acebrón, L. L. Bonilla, C. J. Pérez Vicente, F. Ritort, and R. Spigler, *Rev. Mod. Phys.* **77**, 137 (2005).
- [6] F. Dörfler and F. Bullo, *Automatica* **50**, 1539 (2014).
- [7] F. A. Rodrigues, T. K. D. M. Peron, P. Ji, and J. Kurths, *Phys. Rep.* **610**, 1 (2016).
- [8] I. Z. Kiss, Y. Zhai, and J. L. Hudson, *Science* **296**, 1676 (2002).
- [9] J. Buck, *Quart. Rev. Biol.* **63**, 265 (1988).
- [10] R. A. Oliva and S. H. Strogatz, *Int. J. Bifurcat. Chaos* **11**, 2359 (2001).
- [11] J. Javaloyes, M. Perrin, and A. Politi, *Phys. Rev. E* **78**, 011108 (2008).
- [12] G. Filatrella, A. H. Nielsen, and N. F. Pedersen, *Eur. Phys. J. B* **61**, 485 (2008).
- [13] M. Rohden, A. Sorge, M. Timme, and D. Witthaut, *Phys. Rev. Lett.* **109**, 064101 (2012).
- [14] F. Dörfler, M. Chertkov, and F. Bullo, *Proc. Natl. Acad. Sci. USA* **110**, 2005 (2013).
- [15] K. Wiesenfeld and J. W. Swift, *Phys. Rev. E* **51**, 1020 (1995).
- [16] K. Wiesenfeld, P. Colet, and S. H. Strogatz, *Phys. Rev. Lett.* **76**, 404 (1996).
- [17] Y. Moreno and A. F. Pacheco, *Europhys. Lett.* **68**, 603 (2004).
- [18] T. Ichinomiya, *Phys. Rev. E* **70**, 026116 (2004).
- [19] J. G. Restrepo, E. Ott, and B. R. Hunt, *Phys. Rev. E* **71**, 036151 (2005).
- [20] A. Arenas, A. Díaz-Guilera, and C. J. Pérez-Vicente, *Phys. Rev. Lett.* **96**, 114102 (2006).
- [21] J. Gómez-Gardeñes, Y. Moreno, and A. Arenas, *Phys. Rev. Lett.* **98**, 034101 (2007).
- [22] J. Gómez-Gardeñes, S. Gómez, A. Arenas, and Y. Moreno, *Phys. Rev. Lett.* **106**, 128701 (2011).
- [23] P. S. Skardal and J. G. Restrepo, *Phys. Rev. E* **85**, 016208 (2012).
- [24] P. S. Skardal, J. Sun, D. Taylor, and J. G. Restrepo, *Europhys. Lett.* **101**, 20001 (2013).
- [25] M. Timme, *Phys. Rev. Lett.* **98**, 224101 (2007).
- [26] L. Arola-Fernández, A. Díaz-Guilera, and A. Arenas, *Phys. Rev. E* **97**, 060301(R) (2018).
- [27] M. Brede, *Phys. Lett. A* **372**, 2618 (2008).
- [28] L. Buzna, S. Lozano, and A. Diaz-Guilera, *Phys. Rev. E* **80**, 066120 (2009).
- [29] D. Kelly and G. A. Gottwald, *Chaos* **21**, 025110 (2011).
- [30] P. S. Skardal, D. Taylor, and J. Sun, *Phys. Rev. Lett.* **113**, 144101 (2014).
- [31] R. S. Pinto and A. Saa, *Phys. Rev. E* **92**, 062801 (2015).
- [32] B. Li and K. Y. Michael Wong, *Phys. Rev. E* **95**, 012207 (2017).
- [33] Y. Zou, R. Wang, and Z. Gao, *Physica A* **548**, 122956 (2020).
- [34] V. Khramenkov, A. Dmitrichev, and V. Nekorkin, *Chaos Solitons & Fractals* **152**, 111373 (2021).
- [35] F. Alderisio and M. Bernardo, 2018 17th European Control Conference (ECC) (2018), doi: 10.23919/ECC.2018.8550557.
- [36] P. S. Skardal and A. Arenas, *Sci. Adv.* **1**, e1500339 (2015).
- [37] C. Xu, J. Gao, S. Boccaletti, Z. Zheng, and S. Guan, *Phys. Rev. E* **100**, 012212 (2019).
- [38] P. Erdos and A. Renyi, *Publicationes Mathematicae* **6**, 290 (1959).
- [39] R. Phogat, S. Sinha, and P. Parmananda, *Phys. Rev. E* **101**, 022216 (2020).
- [40] R. Phogat, A. Ray, P. Parmananda, and D. Ghosh, *Chaos* **31**, 041104 (2021).
- [41] A. Ben-Israel and T. N. E. Grenville, *Generalized Inverses* (Springer, New York, 1974).